Chirp Selection and Data Compression for Spaceborne Wide-Swath SAR in FScan-Mode

Rolf Scheiber[a], Michele Martone[a], Nicola Gollin[a]
[a] German Aerospace Center (DLR), D-822234 Wessling, Germany

Abstract

FScan has recently been proposed by Airbus DS as an appealing option to implement high-resolution wide-swath (HRWS) spaceborne SAR imaging [1]. The concept uses the fanning-out beam pointing characteristic of phased array antennas operated at high bandwidth in a favorable way to steer the beam over a much wider swath as the nominal beamwidth would correspond. This paper treats the transmit pulse chirp length as a trade-off parameter and consequentially derives two variants of the FScan modes. The consequences on echo window length and the benefits of dedicated onboard processing for data volume reduction are discussed. In this context, the advantages of using a transform domain BAQ are pointed out.

1 Introduction

Present day spaceborne SAR sensors use the ScanSAR and TOPS modes to perform wide swath imaging of 100-400 km at rather modest azimuth resolution of 10 m to 40 m. Future high-resolution wide swath (HRWS) sensors are designed to overcome this limit by implementing new operation concepts like SCORE [2] and/or multiple azimuth phase centers (MAPS) [3]. Optionally, the echoes of several beams may be received in parallel, covering the wide swath in an effective way without relying on bursts. To circumvent blind ranges corresponding to transmit pulse events, variable PRI settings may be operated, as e.g. in the staggered SAR [4] or slow PRI variation modes. Future SAR sensors will also be able to provide very high resolution in the sub-meter range. The inherent very high bandwidth can alternatively be used to facilitate wide swath mapping [1], [5]. The multi-frequency sub-pulse (MFSP) mode proposed in [5] uses sub-pulses within the same PRI, occupying disjoint range frequency bands to simultaneously image multiple sub-swaths. In contrast, the FScan mode illuminates a wide swath with a continuously changing center frequency. Here, the proper selection of the chirp modulation allows for a drastic reduction of the echo window length [1], at the expense of potentially large chirp durations. This trade-off is discussed in the first part of this paper. The second part introduces a concept for improved onboard data volume reduction based on transform domain block adaptive quantization (BAQ), named block-frequency BAQ, BF-BAQ. Dedicated simulations are conducted which verify the validity of the proposed approach.

2 Chirp Length Dependency

In FScan mode, the chirp length can be treated either as a pure input determined by traditional trade-offs between instrument duty cycle and desired noise equivalent sigma zero (NESZ) or it can be considered as a FScan design parameter to ensure the relevant high SNR contributions across the whole swath to arrive at the receiver quasi simultaneously (see Figure 1). This section describes the basic dependency between the chirp length and the swath width and discusses its implications.

2.1 Time Frequency Diagrams

In Figure 2, the time-frequency diagrams of stripmap and FScan modes are presented for comparison, illustrating the potential for echo window length reduction. The grey area represents the time frequency support of one range line. For better clarity of the concept, the change of the center frequency is assumed proportional to travel time/slant range, even though this is not perfectly true in practice, and an additional modulation is present also due to topography. However, this non-linearity is absorbed by the oversampling of the radar.

For minimizing the echo window length, the radar system must operate with very large chirp lengths, proportional to the intended swath width (**fully overlapped FScan mode**):

$$\tau_{ch,full} = \frac{2(r_{far}-r_{near})}{c_0\left(1-\frac{B_{img}}{B_{Tx}}\right)} = \frac{T_{swath}}{1-\frac{B_{img}}{B_{Tx}}}, \quad (1)$$

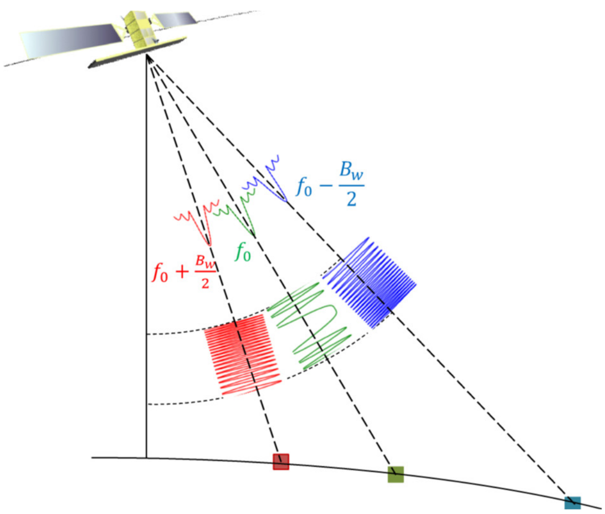

Figure 1 The FScan principle: different targets across the swath are illuminated by different frequencies, whilst echoes arrive simultaneously at the antenna.

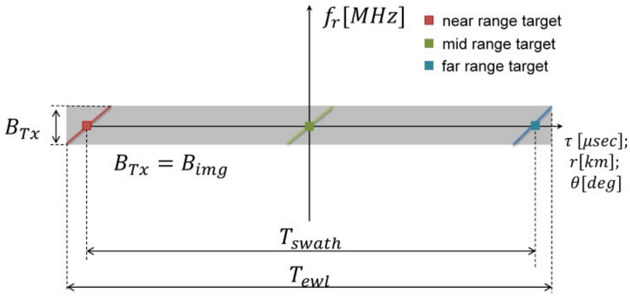

(a) stripmap mode

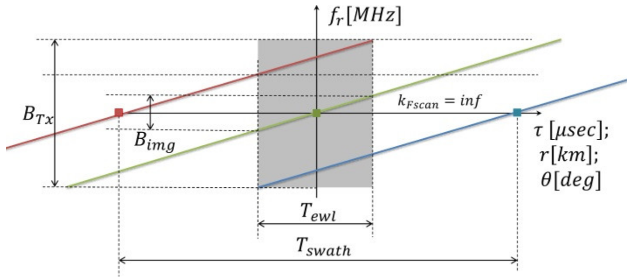

(b) fully overlapped FScan mode

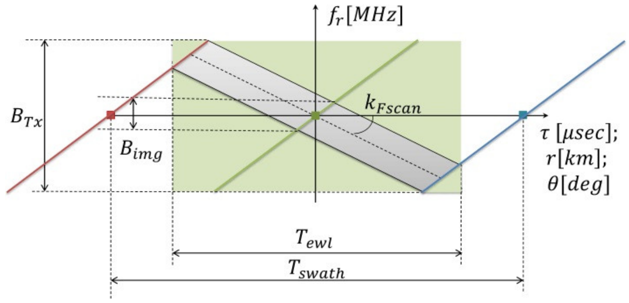

(c) fixed chirp length FScan mode

Figure 2 Time-frequency diagrams of near, mid and far range targets in stripmap (a) and FScan modes. The minimization of the echo window length is achieved with large chirp length: **fully overlapped FScan mode** (b), whereas a trade-off exists between chirp length and echo window length: **fixed chirp length FScan mode** (c).

where T_{swath} is the desired swath width (converted to two-way travel time), B_{Tx} is the bandwidth of the transmitted chirp and B_{img} is the fractional part of it, determined by the Fscan operation of the sensor/antenna, and directly responsible for the range resolution of the SAR image. The echo window length is $T_{ewl} = B_{img}/k_r$, with k_r the modulation rate of the chirp. This mode is illustrated in Figure 2(b), whilst the stripmap case is shown for comparison in Figure 2(a).

Alternatively, if such large chirp durations τ_{ch} are not practically feasible or are limited by the sensor's duty cycle, one may consider the **fixed chirp length FScan mode** in Figure 2(c). The echo window length then becomes:

$$T_{ewl} = T_{swath} - \tau_{ch}\left(1 - 2\frac{B_{img}}{B_{Tx}}\right),\ \tau_{ch} < \tau_{ch,full}$$
$$\text{or} \qquad (2)$$
$$T_{ewl} = \tau_{ch} - T_{swath},\quad \tau_{ch} > \tau_{ch,full}$$

In this case, the time-frequency signal support (grey area) becomes smaller than the area spanned by the echo window length (EWL) and the sampling frequency (green), i.e. oversampling is present and data reduction possibilities should be evaluated.

The parameters in Table 1 are assumed for quantitative evaluation of a potential FScan system in TerraSAR-X-like orbit. The desired azimuth resolution of 1 m calls for a Doppler bandwidth of at least 7000 Hz. With 4 azimuth channels the PRF can be reduced to below 2000 Hz. Taking these parameters, one can compute chirp durations and echo window lengths for the different modes depicted in Figure 2. The evaluation for an 80 km swath is presented in Figure 3, demonstrating the considerable reduction of the EWL compared to the traditional stripmap mode.

Table 1: FScan parameters [1]

Parameter	**Value**
Center frequency	9.8 GHz
Transmit bandwidth B_{Tx}	1200 MHz
Target bandwidth B_{img}	300 MHz
Orbit height	514 km
Number of azimuth channels	4
Azimuth resolution	1 m

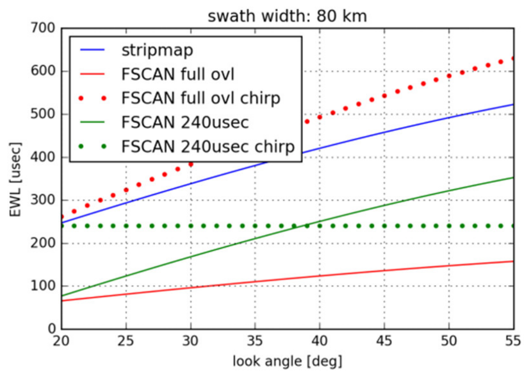

Figure 3 Echo window lengths EWL (solid lines) and chirp durations (dotted lines) for an 80km wide swath and sensor operation in stripmap (see Figure 2(a), in blue), fully overlapped FScan mode (see Figure 2(b), in red) and for a fixed 240 µsec chirp FScan mode (see Figure 1(c), in green). The required/assumed chirp lengths are indicated with dotted lines.

2.2 Timing Diagrams

Whether a specific FScan mode is feasible for a certain look angle and swath width can be assessed by the analysis of the timing diagram. Figure 4 presents examples for the EWL corresponding to 30 km and 80 km swath width at 39° look angle. Transmit events are colored in green, whereas the nadir echo is shown in red. Due to the large pulse durations in FScan mode, the choice of suitable PRF settings might become restricted. Feasible echo window positions are marked in blue. The 30 km stripmap case corresponds to TerraSAR-X coverage. The same coverage can be easily achieved with the fully overlapped FScan mode, resulting in a chirp length of 181 µsec according to (1). The EWL is minimized in this case to 45 µsec. The fixed chirp length case requires a larger EWL of 104 µsec. On the other hand, the 80 km swath turns out to be unfeasible in traditional stripmap mode (expected), but also in the fully overlapped FScan case (chirp length of 483 µsec would be required, which fills the timing diagram completely), whereas in a fixed chirp length FScan mode, such high coverage becomes possible for two PRF settings (1750 Hz and 2050 Hz). The presented case assumes a 240 µsec chirp and results in a comparable EWL of 242 µsec.

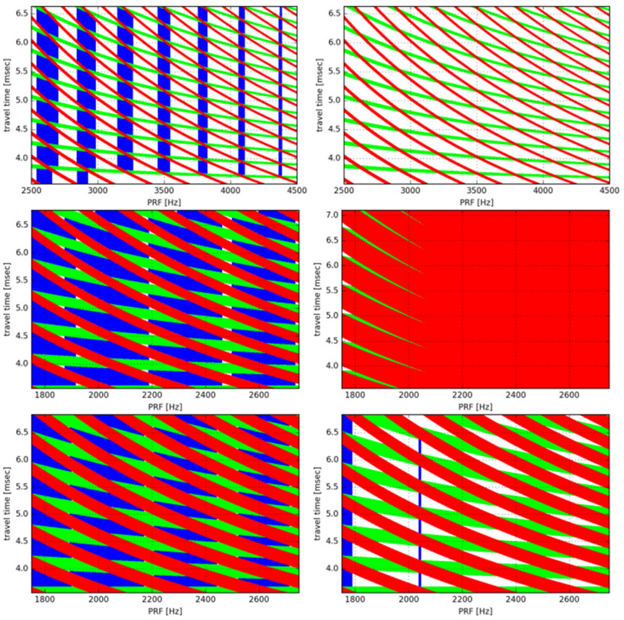

Figure 4 Timing diagrams for a 30km (left) and 80km (right) swath at 39° look angle in stripmap mode (top), fully overlapped FScan mode (middle) and 240µsec chirp length FScan mode (bottom).

3 Dedicated Onboard Processing

Although the fixed chirp length FScan mode in Figure 2(c) does not minimize the EWL, it is possible to considerably reduce the data amount for downlink by means of onboard processing. Three possible onboard implementations are reported, two featuring a deramping operation and one featuring a block-wise FFT. The first two are described in the following subsection 3.1 while the latter in subsection 3.2.

3.1 Employment of Deramping Operation

Independently of the FScan chirp parameterization, the sensor's ADC needs to sample the data with a rate higher than the transmit pulse bandwidth B_{Tx} in order to avoid aliasing effects. In fixed chirp length mode, the time frequency support is not completely filled (as seen in Figure 2(c)) and a deramping operation followed by low-pass filtering and decimation can achieve an overall bandwidth and thus data sample reduction. One should notice that this reduction is less than the ratio of chirp and target bandwidth, as the target bandwidth B_{img} will be increased by an amount proportional to the FScan rate k_{FScan}.

$$B_{img,FScan} = B_{img} \cdot \left(1 + \frac{k_{FScan}}{k_r}\right), \qquad (3)$$

with

$$k_{FScan} = \frac{B_{Tx} - B_{img}}{T_{swath} - \tau_{ch}\left(1 - \frac{B_{img}}{B_{Tx}}\right)}. \qquad (4)$$

The resulting number of EWL samples is shown in Figure 5, where an oversampling factor of 20% has been assumed. For chirp lengths approaching the fully overlapped FScan case (right end of each line), the EWL becomes minimum and the benefits of onboard processing start to diminish.

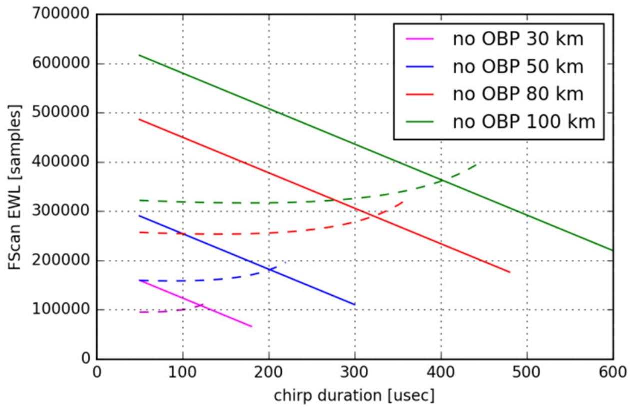

Figure 5 Effective window lengths as a function of chirp duration. Onboard processing (dashed lines) offers data reduction possibilities up to 45% for shorter chirp length.

3.1.1 Onboard Implementation Options

The onboard implementation of the deramping is performed by a complex phase multiplication at range line level. Then two options are possible for data reduction (see Figure 6 (left) and (middle)): (1) a low pass (LP) FIR filter is implemented, followed by decimation and traditional BAQ. (2) LP filtering is performed as part of a FFT-BAQ, which allocates zero bits to the high frequency spectral parts [6, 7], which do not carry any information (run length encoding).

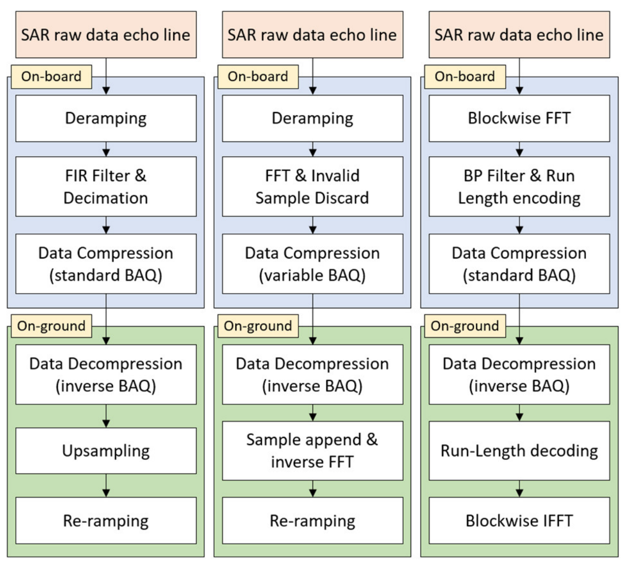

Figure 6 Concepts for onboard data volume reduction. FIR filter, decimation and traditional BAQ (left). FFT, sample discard and variable bit BAQ (center). Block-wise FFT with BP filter and BAQ in frequency domain (right).

Out of these two options, the second one is preferred:

- In the fully overlapped FScan mode, the traditional BAQ completely loses its adaptiveness with target range, as all targets overlap (see Figure 2(b)). A transform domain BAQ is a better choice for data compression, in this particular case without the need neither for deramping nor for applying blocks in time domain. Adaptiveness to targets is completely achieved in frequency domain.
- In the fixed chirp FScan mode, adaptiveness is possible with blocks in time and frequency domain with allocation of different bits in frequency domain.

Considering now the need for floating point operations for the deramping, the FFT option would not impose a considerable larger computational effort having the advantage of improved BAQ compression and LP filter performance. However, feasibility depends on available HW resources and trade-off analyses are still to be conducted once the mission mode design - including the FScan parametrization in terms of chirp length - has been completed.

3.2 Block-wise FFT BAQ (BF-BAQ)

In this section, another approach has been investigated, with the goal of achieving a more efficient data volume reduction capability. The basic idea is to avoid the quantization of the whole signal support (i.e. the green area in Figure 2(c)), but only of those components which are actually received after the FScan operation. For doing that, we introduce a novel quantization method called Block Frequency BAQ (BF-BAQ), which can be summarized with the block scheme on the right-hand side of Figure 6.

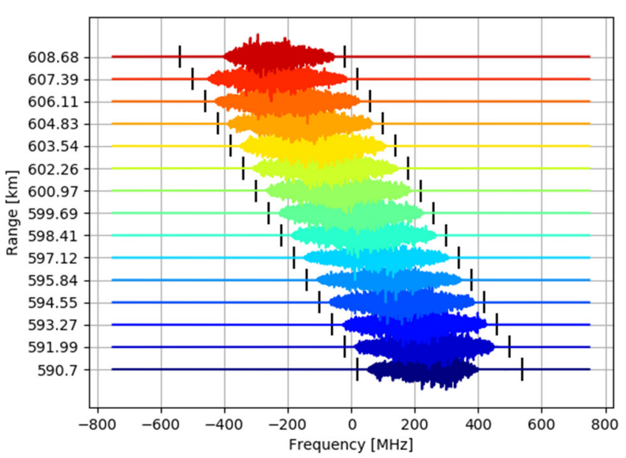

Figure 7 Example of a block-wise operation on the EWL signal in frequency domain: the x axis represents the bandwidth and each single colored line represent one block (in this case, $N_b = 15$ blocks are considered), while the y-axis represents the range position of the block before the FFT operation. For each block, the two small black vertical lines represent the boundary for applying the run-length coding (i.e. number of zero bit encoded samples, outside the two lines) and for operating the BAQ (between the two lines).

The BF-BAQ consists of an arbitrary division in blocks of the EWL signal and an independent FFT operation for each of the blocks. According to the FScan theory, the target signal is concentrated in a specific bandwidth portion as function of the range position, i.e. as the range position of a targets increases, they are associated to lower frequencies within the overall spectrum. By performing an FFT operation of a small part of the EWL signal (one block) we are able to isolate the target information on a few samples, thus excluding the useless part of the target with a simple run-length coding. A visual example of the target information dependency on frequency is reported in Figure 7, where $N_b = 15$ blocks have been considered. It is clear that the target information is bounded to a smaller number of samples (approximatively one third) with respect to the whole range line extension. From this representation, quantizing only the relevant part of the block is quite straightforward, hence, we discard those samples which lie outside of the informative frequency support. A key aspect of this quantization method is the fact that, by performing a run-length of the non-informative samples, we can encode the samples with a given bitrate, thus maintaining the required representation accuracy while reducing the overall needed memory for one range line.

3.2.1 Encoding Performance: SQNR

The Signal-to-Quantization Noise Ratio (SQNR) is a well-established performance metric to assess the impact of quantization errors, and can be easily related to the coherence or the interferometric phase noise in SAR images. It is defined as the power ratio between the noise-free SAR data I and the quantization error $q = I - \hat{I}$:

$$\boldsymbol{SQNR} = \frac{\sum_{s=1}^{S} |I_s|^2}{\sum_{s=1}^{S} |q_s|^2} \tag{5}$$

where S represents the total number of considered samples.

3.2.2 Data Volume Reduction

The amount of data volume reduction $\boldsymbol{DR}_{\%}$ is estimated by means of signal encoding quality comparison, i.e. we expect to reach the same encoding quality of the BAQ which operates at a higher average bitrate. It is calculated as follows:

$$\boldsymbol{DR}_{\%} = \frac{(1 - B)}{B_{eq}} \cdot 100 \tag{6}$$

where B represents the average bitrate of the BF-BAQ and B_{eq} represents the bitrate of the BAQ achieving the same SQNR encoding performance.

3.2.3 Computational Complexity

Another relevant aspect concerns the amount of resulting computational effort to be considered onboard for the implementation of the proposed BF-BAQ. This is typically defined as the number of floating-point operations, represented by $\boldsymbol{O}$. We will compare the computational complexity of the BF-BAQ to the second technique proposed in Figure 6, which consists of full range line FFT, sample discard and variable bit BAQ, claiming a sample reduction up to 45 % (see Figure 5). We want to point out the advantage of performing multiple smaller FFTs with respect to a

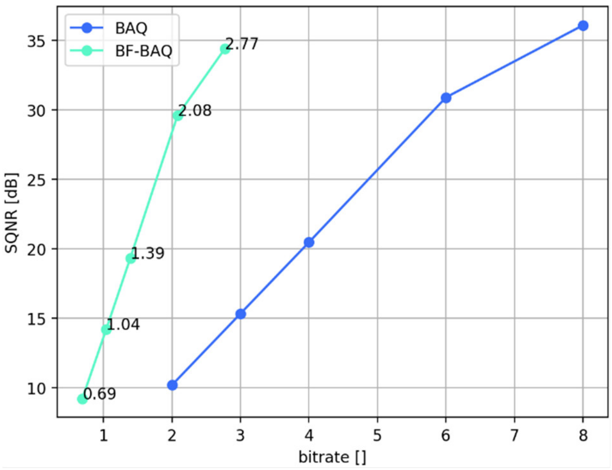

Figure 9 SQNR for BAQ and BF-BAQ with 15 blocks as function of overall average bitrate. The BAQ at 8 bits is a uniform ADC, therefore the gain w.r.t. the 6 bits BAQ is lower than expected (every bit more is translated to a gain of about 6 dB for the BAQ). Due to the employment of run-length coding in frequency domain, the overall average bitrate for the BF-BAQ is fractional and it is reported at the corresponding value with a label.

single FFT on the whole signal. For a N_s-point FFT, the computational complexity is denoted as

$$\mathcal{O}_{FFT} = N_s \log N_s \, . \tag{7}$$

If multiple blocks are considered instead of the full EWL signal of N_s samples, the computational complexity becomes:

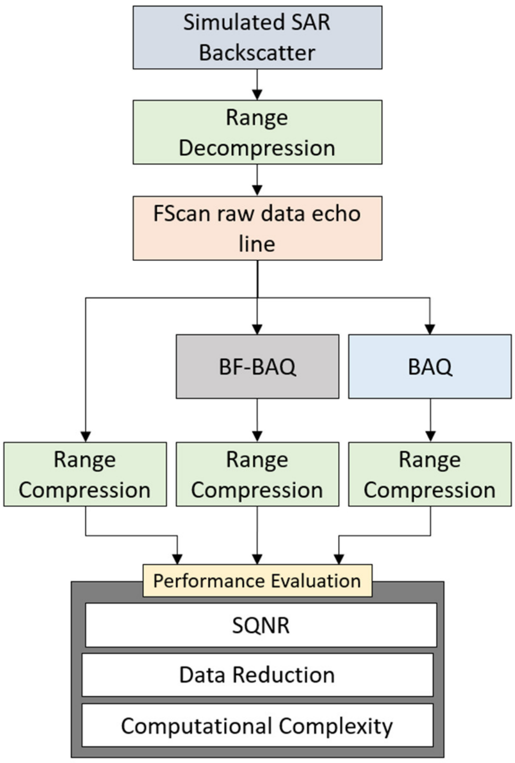

Figure 8 Block scheme of the simulator used for the performance evaluation. The FScan data is encoded and decoded through BF-BAQ and standard BAQ in time domain and the encoding metrics are derived after the range compression in the Performance Evaluation block.

$$\mathcal{O}_{B-FFT} = N_s \log \frac{N_s}{N_b} \, , \tag{8}$$

where N_b is the number of considered blocks. From this latter expression it is clear that the computational complexity is lower with respect to the other approach featuring the full range line FFT. Moreover, the reference technique implements onboard deramping as well, which adds more computations, and has not been considered in the calculations.

We refer to the computational complexity reduction as

$$\mathrm{CC}_{R\%} = 100 - \frac{\mathcal{O}_{B-FFT} \cdot 100}{\mathcal{O}_{FFT}} \, . \tag{9}$$

3.3 Simulation Result

In order to assess the encoding capabilities of the previously introduced BF-BAQ, a dedicated FScan simulator has been developed. It consists of a FScan range line generator through inverse focusing of a distributed target. The considered mode assumes a fixed length chirp. Two different quantization methods are investigated: BF-BAQ and a standard BAQ operating in time domain.

The encoding sample bitrate is considered equivalent for both techniques, even though it is worth to recall that the overall bitrate will be lower for the BF-BAQ. This is due to the fact that the employment of run-length coding discards many samples of the received FScan range line, hence reducing the number of samples.

The block scheme of the simulator is reported in Figure 8. An uncompressed version of the range line is kept through the quantization process in order to estimate the SQNR, according to (5).

The considered bitrate for encoding the samples is the same for both techniques (e.g. BF-BAQ at 1.04 average bitrate is employing a 3-bit BAQ on the samples). The comparison of the two different quantization methods can be done by comparing the BF-BAQ technique with the BAQ equivalent fractional bitrate achieving the same SQNR [9].

The summary of the simulation results is reported in Table 2. Different number of blocks have been considered, suggesting that the higher the number of blocks is, the higher the capabilities of the technique will be for reducing the overall bitrate and the computational complexity. The "Bitrate" column refers to the number of bits employed for

Table 2: Summary performance results for the investigated cases of BF-BAQ.

Blocks	Bitrate [bps]	Avg. Bitrate [bps]	BAQ Eq. [bps]	$DR_{\%}$ [%]	$CC_{R\%}$ [%]
5	3.00	1.20	2.8	57.14	13.23
5	4.00	1.60	3.8	57.89	13.23
10	3.00	1.08	2.8	61.43	18.92
10	4.00	1.44	3.8	62.11	18.92
15	3.00	1.04	2.8	62.86	22.25
15	4.00	1.39	3.8	63.48	22.25
20	3.00	1.02	2.8	63.57	24.62
20	4.00	1.36	3.7	63.24	24.62
25	3.00	1.01	2.8	63.93	26.45
25	4.00	1.34	3.7	63.78	26.45

each sample, while the "BAQ Eq." column refers to the required bitrate for a direct BAQ for achieving the same encoding performance of the BF-BAQ. The data volume reduction factor is derived by considering this latter bitrate as reference as described in Section 3.2.3. The computational complexity reduction is computed in comparison to a full range line FFT operation (as proposed in Figure 6) and derived in Section 3.2.1.

4 Conclusions

This paper presented the chirp length as a trade-off parameter for defining the FScan mode and in consequence the echo window length of the recorded range lines. For shorter swath widths, the fully overlapped FScan mode can minimize the echo window length. However, for large swath width, timing constraints might ask for an upper bounded fixed chirp length. In the latter case, dedicated onboard processing was shown to be beneficial for decreasing the data amount for downlink. We argue that a state-of-the-art time domain BAQ loses adaptivity with target range in FScan mode in general, and we propose a transform domain block-wise FFT BAQ for better compression performance at slightly larger computational cost. The proposed BF-BAQ shows a superior performance in terms of data volume reduction and computational effort with respect to alternative techniques. The significant data reduction of about 64% is much higher than the compression rates of the techniques exploiting deramping (best case of 45%). We are confident that there is further room for improvement, especially in the boundary level decision, leading to the expectation of an even higher compression rate. Future performance assessments will include analysis on targets with different brightness as well as a FScan 2D SAR scene simulation.

Acknowledgment

This work receives funding from the EU's Horizon 2020 research and innovation programme under grant agreement No 822014. The authors acknowledge their colleagues Gerhard Krieger and Alberto Moreira for initial discussions on the topic of this paper.

5 Literature

[1] Ch. Roemer: "Introduction to a new wide area SAR mode using the F-Scan principle" Proc. IGARSS, 2017

[2] M. Suess, B. Grafmueller, R. Zahn: A novel high resolution, wide swath SAR system, in Proc. IGARSS, Sydney, Australia, 2001.

[3] N. Gebert, G. Krieger and A. Moreira: Digital Beamforming on Receive: Techniques and Optimization Strategies for High-Resolution Wide-Swath SAR Imaging, in IEEE Trans. Aerosp. Electron. Syst., vol. 45, no. 2, pp. 564-592, 2009.

[4] M. Villano, G. Krieger and A. Moreira: Staggered SAR: High-Resolution Wide-Swath Imaging by Continuous PRI Variation, in IEEE Trans. Geosci. Remote Sens., vol. 52, no.7, pp.4462-4479, 2014.

[5] F. Bordoni, M. Younis, G. Krieger: Multifrequency Subpulse SAR: Exploiting Chirp Bandwidth for an Increased Coverage, IEEE Geoscience and Remote Sensing Letters, vol. 16, no. 1, pp. 40-44, 2018.

[6] U. Benz, K. Strodl, and A. Moreira, "A Comparison of Several Algorithms for SAR Raw Data Compression," IEEE Transactions on Geoscience and Remote Sensing, vol. 33, pp. 1266–1276, Sep. 1995.

[7] J. Fischer, U. Benz, A. Moreira: "Efficient SAR Raw Data Compression in Frequency Domain", Proc. IGARSS, 1999

[8] M. Martone, M. Villano, M. Younis and G. Krieger, "Efficient Onboard Quantization for Multichannel SAR Systems," in IEEE Geoscience and Remote Sensing Letters, vol. 16, no. 12, pp. 1859-1863, Dec. 2019, doi: 10.1109/LGRS.2019.2913214.

[9] M. Martone, B. Bräutigam and G. Krieger, "Azimuth-Switched Quantization for SAR Systems and Performance Analysis on TanDEM-X Data," in IEEE Geoscience and Remote Sensing Letters, vol. 11, no. 1, pp. 181-185, Jan. 2014, doi: 10.1109/LGRS.2013.2251603.